

Manuscript ID

ZUMJ-2203-2537 (R1)

DOI

10.21608/zumj.2022.129544.2537

ORIGINAL ARTICLE

Cytoarchitecture Changes of the Rat Thyroid Gland Following Furan Administration Implemented Fas-Apoptotic Pathway with Potential Abrogating Role of SeleniumDalia A. Mandour^{1*}, Marwa Tharwat², Doaa M. Shuaib³, Rasha Mohammed Sabry⁴^{1, 2, 4}Human Anatomy and Embryology Department, Faculty of Medicine, Zagazig University, Egypt.³Human Anatomy and Embryology Department, Faculty of Medicine, Cairo University, Egypt

ABSTRACT

***Corresponding author :**Dalia A. Mandour
Human Anatomy and
Embryology Department,
Faculty of Medicine, Zagazig
University, Egypt E-mail:
daliemandour@zu.edu.eg

Submit Date 2022-03-25 19:10:05

Accept Date 2022-03-28 20:24:15

Background: Furan, a cytotoxic chemical produced during thermal processing of foods, is an endocrine disruptor that induces injury of most endocrine glands. The aim of this study is To evaluate the effects of furan exposure on cytoarchitecture of the rat thyroid gland and to assess the potential protective role of selenium (Se).**Methods:** Twenty-four male Sprague Dawley rats were allocated into four groups and gavaged daily for 4 weeks. I (Control group) received corn oil, II (Se group) received selenium (1µg/100g bw/day), III (Furan group) received furan (40 mg/kg bw/day), and IV (Furan/Se group) received furan and Se simultaneously. Serology was performed and Paraffin sections of thyroid gland were processed for staining by H&E and Periodic Acid Schiff (PAS). Also, immunohistochemical study was carried out for detection of Fas protein and the proliferating cell nuclear antigen (PCNA). Moreover, morphometric analysis was performed.**Results:** Furan group exhibited discernible histopathological changes in the thyroid gland; outcomes associated with depleted thyrocolloid and decreased its mean area % and extensive immunoexpression of Fas and PCNA with increased their mean area %. In addition, furan group displayed increased serum malondialdehyde (MDA), interleukin-1 β (IL-1β), tumour necrosis factor alpha (TNF-α), and thyroid stimulating hormone (TSH) but serum reduced glutathione (GSH), glutathione peroxidase-1 (GPX-1) activity, and serum total T3, T4 were decreased. Co-supplementation of Se with furan partially ameliorated the histological, immunohistochemical and biochemical changes.**Conclusion:** Furan induced deleterious effects on rat thyroid gland that mediated mostly via induction of oxidative, inflammatory and Fas apoptotic pathways; resultants that were abrogated by Se.**Keywords:** Furan, Fas, thyroid-histopathology, selenium, rats.

INTRODUCTION

Currently, heat-induced food contaminants have attracted the scientific concern due to their adverse effects on human health. Furan is one of the most known toxic heat-induced food contaminants [1]. Furan is formed during heat-processing of foods as cooked, canned, jarred and baby foods, infant formula, cereals products, meat, sauces and a variety of beverages such as coffee [2,3,4]. Furan is also produced following thermal degradation of carbohydrates, ascorbate,

unsaturated fatty acids, and carotenes [1,5]. In manufacturing industry, furan is used in the production of organic-based compounds as lacquers, resins, insecticides, stabilizers, and some pharmaceuticals [6]. In addition, furan and its derivatives are used as flavoring agents in some foods and in tobacco products [7].

Human exposure to furan is unavoidable because of its widespread persistent and extensive commercial use. Furan commonly leaches into the environment from industrial raw materials and

from the furan-containing thermally processed foods. Besides, it is widely spread as a main constituent of wood smoke, cigarette smoke, and exhaust engine gases in the environment [8]. Following oral exposure, furan easily permeated through biological membranes, and is rapidly absorbed from the gastrointestinal tract, and metabolized mainly by the liver [9].

Furan was reported to induce injury of many organs and tissues in rodents including; the liver [10], brain [11], kidney [12], and heart [13]. Also, furan was considered by National Toxicology Program (NTP) [14] and International Agency for Research on Cancer (IARC) [15] as "a possibly carcinogenic to humans". The proposed mechanisms by which furan exposure caused such tissue injury are the oxidative stress and the induction of tissue inflammation [16-18]. Furthermore, emerging evidence implicated furan as one of the endocrine disruptors [19]. It disturbs the adrenal gland and pancreas [20], spleen and thymus [13], and the reproductive system [8, 19]. Recently, a number of clinical supplementation trials of Se have indicated its positive effects on health status of the individuals. Plant-derived foods that are relatively rich in Se include Brazil nuts, legumes, cruciferous vegetables, and bulb vegetables. Also, animal-derived foods containing adequate amount of Se involve meat, eggs, and fish. The recommended daily Se intake for adults is 60–70 µg [21]. Importantly, Se supplementation is recommended in a variety of thyroid pathologies owing to its crucial role in thyroid hormones (THs) biosynthesis and it is a potent antioxidant that protects the follicular cells from damage by free radicals [22]. In addition, Se is an essential trace element that combats inflammation of thyroid and maintains the integrity of its cells [23].

Despite the furan's endocrine disruption potentiality, it was strikingly noted that there is a paucity of information in the published literature about its toxicological effects on the thyroid gland. Therefore, this study was undertaken firstly to evaluate the histopathological changes of the rat thyroid gland following chronic oral furan administration and validate the role of Se in counteracting these detrimental effects of furan.

METHODS

Chemicals

Furan (C₄H₄O, Cat#185922 and CAS no. 110-00-9, ≥99% pure) was purchased from Sigma Aldrich Chemical Co. (St. Louis, MO, USA). It was dissolved in corn oil. The used dose of furan in this experiment was (40 mg/kg bw/day) and it was selected on the basis of a sub-chronic

exposure dose in rats that was adopted by Rehman et al. [8].

Selenium sodium selenite was purchased from Sigma Aldrich Chemical Co., (St. Louis, MO, USA). It was dissolved in distilled water.

Experimental design

Twenty four male adult rats of Sprague Dawley strain aged 3-4 months and weighing 200-250 gm were purchased from the animal house of Zagazig Scientific and Medical Research Center (ZSMRC) at Medical College, Zagazig University. The rats were housed in well-ventilated plastic cages (6 rats per a cage) in a controlled room temperature (22±2°) and 12/12h light/dark cycle and they were allowed standard pellet food and water ad libitum. The rats were left for one week to acclimatize to the lab. conditions before the beginning of the study. The body weight of each rat was recorded weekly during the experiment and the dose of each treatment was adjusted accordingly. All rats were handled and treated in accordance with the standard guidelines for caring of the experimental animals and followed the rules of Institutional Animal Care and Use Committee of Zagazig University.

Animal groups

The rats were randomly categorized into four equal groups:

I (Control group): received 1ml/kg bw/day corn oil as a vehicle for four consecutive weeks.

II (Se group): gavaged with Se sodium selenite (1µg/100g bw/day) for four consecutive weeks [24].

III (Furan-treated group): gavaged with furan (40 mg kg bw/day) for four consecutive weeks [8].

IV (Furan/Se treated group): gavaged simultaneously with Se and furan at the same doses of groups II and III.

Serum and tissue sampling

At the end of dosing period, on day 29, the rats were weighted and fasted overnight and blood samples were withdrawn from the retro-orbital venous plexus of each rat and left to clot at room temperature in non-heparinized tubes; then the collected blood samples were centrifuged at (3000 r.p.m. for 15 min.) to obtain the serum that was stored at -20 °C until the time of biochemical analysis. Afterwards, all rats were euthanized by I.P injection of high dose of the anesthetic sodium pentobarbital (100 mg/kg bw). Then, a longitudinal incision was made in the skin of the neck and the larynx and trachea with the encroached thyroid gland were cut. Immediately, the thyroid gland was dissected and fixed in 10% neutral buffered formalin (NBF) for 48 hours to

be processed later for histological and immunohistochemical studies.

Histological study

The formalin-fixed thyroid gland was dehydrated in the ascending series of ethanol, cleared with xylene and installed in paraffin wax then sectioned at 5 μ m thicknesses using a Leica microtome (RM 2125, Leica Biosystems Nussloch GmbH, Germany). Finally, some sections were stained with Hematoxylin & Eosin (H&E) stain "for a routine histological thyroid examination". Meanwhile, other sections were specially stained with Periodic acid Schiff (PAS) reagent to demonstrate the glycoprotein (thyrocolloid) in the thyroid follicles that appeared bright red/magenta in color [25]. The H&E and PAS-stained sections were inspected under a Leica light microscope (DM-500, Microsystems; AG, Heerbrugg, CH-9435, Switzerland) and photographed using Leica digital camera (ICC50, W camera) in the Department of Human Anatomy and Embryology, Faculty of Medicine, Zagazig University.

Immunohistochemical (IHC) study

Immunostaining of 4 μ m thick paraffin thyroid sections was performed using a standard avidin-biotin peroxidase complex system for detection of Fas antigen (CD95) which is a marker of extrinsic pathway of apoptosis and proliferating cell nuclear antigen (PCNA) which is a marker of proliferation of the cells [26]. Briefly, the paraffin-sections were mounted on positively charged slides then they were deparaffinized in xylene and rehydrated in a descending grades of ethanol. Subsequently, 3% hydrogen peroxide was added to block the endogenous peroxidase activity. Then, the slides were subjected to antigen retrieval and covered immediately with blocking reagent (normal rabbit serum) to suppress non-specific immunoreactions. Afterwards, the sections were incubated at 4°C overnight with PBS-diluted two primary antibodies, viz. polyclonal rabbit anti-Fas antibody (dilution 1:200; Abcam, Cambridge, UK) and monoclonal mouse anti-PCNA antibody (dilution 1:100; Dako, Cytomation, Glostrup, Denmark). Then, the slides were incubated with a link reagent (biotin-labeled secondary antibodies, goat anti-rabbit for Fas and goat anti-mouse for PCNA) followed by labeling reagent (a streptavidin peroxidase). Afterwards, diaminobenzine (DAB) chromogen solution was added to the slides to help visualization of the antigen-antibody interaction. Finally, the slides were counter stained with a Mayer's hematoxylin. Negative control slides were prepared by performing the same previous steps with replacing the primary antibodies

with PBS. Positive immunostaining was identified under the light microscope by visualizing cell membrane brown staining for positive Fas reactions and nuclear brown staining for positive PCNA reactions.

Histomorphometric analysis

The mean area % of the thyrocolloid of the thyroid follicles in PAS-stained sections and the mean area % of Fas and PCNA-positive immunoreactivity in IHC-stained sections in six non-overlapped high power fields (\times 400) from rats in each group were morphometrically analyzed using Image J analyzer computer system (Wayne Rasband, NIH, Bethesda, Maryland, USA). The obtained data from each group were quantitatively presented as Mean \pm SD and statistically analyzed.

Biochemical analysis

Measurement of lipid peroxidation

Serum malondialdehyde (MDA; an indicator of lipid peroxidation) was determined spectrophotometrically using thiobarbituric acid reactive substances (TBARS) assay kit (Sigma-Aldrich, MO, USA). MDA was expressed as (nmol/ml).

Measurement of antioxidant enzymes

Serum reduced glutathione (GSH) and Glutathione peroxidase-1 (GPX-1) were measured spectrophotometrically using a commercial assay kits (Biodiagnostic, Egypt). GSH was expressed as (nmol/L) and GPX-1 was expressed as (U/ml).

Measurement of the pro-inflammatory cytokines

Serum IL-1 β and TNF- α were measured Using rat ELISA kits following the manufacturer's instructions. Both markers were expressed as (pg/ml).

Measurement of serum thyroid hormones

Serum total triiodothyronine (T3), thyroxine (T4) and thyroid stimulating hormone (TSH) were assessed using the rat ELISA assay kits, provided by Calbiotech Inc. (California, USA) following the manufacturer's instructions

Statistical analysis

Morphometric data and the data of biochemical assay were expressed as Mean \pm SD. They were analyzed using the statistical package for the social sciences (SPSS, version 20; IBM, Chicago, Illinois, USA). Statistical analysis was performed using one-way analysis of variance (ANOVA) followed by Tukey's multiple comparison post hoc test for pairwise comparison. The level of significance was set at P value less than 0.05[27].

RESULTS

No mortalities were recorded in the animals of different groups throughout the whole study

period. However, a mild reduction in the activity was observed in the furan-treated rats.

Histological results

Results of Hematoxylin and Eosin (H&E) staining

The group I (control group) and group II (Se group) displayed a similar histological picture of normal thyroid lobules that exhibiting multiple follicles of variable sizes; large peripheral follicles and small central ones. These thyroid follicles were surrounded by connective tissue enclosing a normal amount of interfollicular cells, blood capillaries and nerve fibers. Each follicle was composed of a single raw of follicular epithelial cells that appeared flat or cuboidal in shape having basophilic cytoplasm with spherical vesicular nuclei and surrounding a central colloid-filled lumen (Fig.1a,d).

The group III (Furan group) revealed shrunken thyroid lobules that exhibiting collapsed follicles with little colloid and surrounded by connective tissue enclosing a large amount of interfollicular cells, congested blood capillaries and focal areas of hemorrhage. Most of the follicles displayed multiple layers of follicular cells, other follicles displayed disruption of their basal lamina with focal loss of epithelial cells and communication with the adjacent follicles (Fig.1b,e).

The group IV (Furan/Se group) disclosed many follicles were distended with colloid and few follicles had little amount. The surrounding connective tissue revealed no congestion in blood capillaries and a moderate amount of interfollicular cells. Some follicles revealed arranged epithelial cells in a single layer while others showed focal areas of follicular cell proliferation (Fig.1c,f).

Results of Periodic Acid Schiff (PAS) staining

The control and Se groups exhibited extensive PAS-positive reaction in the colloid and basement membranes of almost all thyroid follicles (Fig. 2a). On the contrary, thyroid sections of the furan group revealed PAS-positive reaction in few follicles having small amount of colloid and also in the discontinuous basement membranes of some disrupted follicles (Fig. 2b). The Furan/Se group displayed PAS-positive reaction in the colloid and basement membranes of most follicles (Fig. 2c).

Immunohistochemical results

Results of Fas immunostaining

The control and Se groups disclosed a weak Fas immunostaining in the cell membranes of few follicular cells (Fig. 3a). Meanwhile, thyroid sections of the furan group displayed an extensive Fas immunostaining in the cell membranes of

many follicular cells (Fig. 3b). The Furan/Se group revealed a moderate Fas immunostaining in the cell membranes in a small number of follicular cells (Fig. 3c).

Results of PCNA immunostaining

The control and Se groups displayed PCNA-negative immunoreactivity in most nuclei of the follicular cells with weak PCNA-positive immunoreactivity in few nuclei of other follicular cells (Fig. 4a). On the other hand, the furan group revealed a prevalent PCNA-positive immunoreactivity in numerous nuclei of the follicular epithelium (Fig. 4b). The Furan/Se group disclosed PCNA-positive immunoreactivity in a small number of nuclei of the follicular epithelium (Fig. 4c).

Histomorphometric results

Furan group exhibited a significant decline ($P<0.0001$) in the mean area % of the colloid of the thyroid follicles in PAS-stained sections compared with the control and Se groups. Co supplementation of selenium with furan in Furan/Se group resulted in a significant increase ($P<0.0001$) in this mean area % compared to the furan group, but still showing a significant difference when compared to the control and Se groups (Fig. 2d).

Furan group demonstrated a significant rise ($P<0.0001$) in the mean area % of Fas immunoexpression in comparison with the control and Se groups. While, Furan/Se group revealed a significant decrease ($P<0.0001$) in this area % compared to the furan group, also there was a significant difference when compared to the control and Se groups (Fig. 3d).

Furan group revealed a statistical significant increase ($P<0.0001$) in the mean area % of PCNA immunoexpression compared to the control and Se groups. In the Furan/Se group, there was a significant decrease ($P<0.0001$) in this mean area % compared to the furan group, while there was a significant difference when compared to the control and Se groups (Fig. 4d).

Biochemical results

Serum MDA, IL-1 β and TNF- α increased significantly ($p<0.0001$) while GSH and GPX-1 decreased significantly ($p<0.0001$) in the Furan group compared to the control and Se groups. In the Furan/Se group, there was a significant decrease in serum MDA, IL-1 β and TNF- α while increase in GSH and GPX-1 as compared to the furan group (Table 1).

Serum total T3 and total T4 decreased significantly ($p<0.0001$) while serum TSH increased significantly ($p<0.0001$) in the Furan group when compared with the control and Se

groups. In the Furan/Se group, there was a significant increase in serum total T3 and Total T4

while a decrease in TSH as compared to the furan group (Table 2).

Table 1. Serum MDA, GSH, GPX-1, IL-1β and TNF-α in all experimental groups.

MDA (nmol/ml)		10.73±1.85	26.85±3.55 ^{ab}	19.16±3.40 ^{abc}	36.24	< 0.0001
GSH (nmol/L)	4.00±0.83	4.70±0.81	1.02±0.17	2.45±0.39	41.76	<0.0001
GPX-1 (U/ml)	2.66±0.40	2.91±0.47	0.92±0.15 ^{ab}	1.57±0.26 ^{abc}	42.79	<0.0001
IL-1β (pg/ml)	23.28±2.98	20.61±3.92	36.08±3.25 ^{ab}	30.16±2.84 ^{abc}	27.17	<0.0001
TNF-α (pg/ml)	20.23±2.08	18.00±2.51	31.45±3.30 ^{ab}	25.80±4.35 ^{abc}	21.47	<0.0001

Number= 6 rats in each group. Values were expressed as Mean±SD. Statistical analysis was carried out using One-way ANOVA followed by Tukey's test. MDA: malondialdehyde; GSH: reduced glutathione; GPX-1: glutathione peroxidase-1, IL-1β: interleukin-1 β, TNF-α: tumour necrosis factor alpha.

- ^a significant p value compared to control group.
- ^b significant p value compared to Se group.
- ^c significant p value compared to furan group.

Table 2. Total free T3, T4 and TSH in all experimental groups .

Total T3 (ng/ml)	1.23±0.25	1.36±0.30	0.15±0.03 ^{ab}	0.67±0.10 ^{abc}	43.12	< 0.0001
Total T4 (ng/ml)	13.48±2.24	11.78±1.24	6.73±0.59 ^{ab}	9.00±0.78 ^{abc}	28.23	<0.0001
TSH (IU/ml)	1.08±0.23	1.13±0.25	7.55±1.23 ^{ab}	3.55±0.46 ^{abc}	119.37	<0.0001

Number= 6 rats in each group. Values were expressed as Mean±SD. Statistical analysis was carried out using One-way ANOVA followed by Tukey's test. T3: triiodothyronine; T4: thyroxine; TSH: Thyroid stimulating hormone.

- ^a significant p value compared to control group.
- ^b significant p value compared to Se group.
- ^c significant p value compared to furan group.

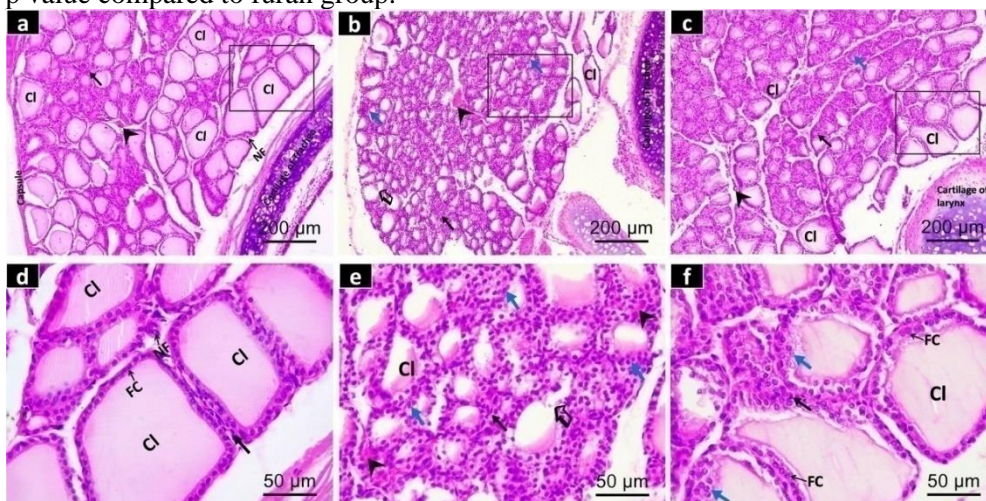


Figure1. Photomicrographs of H&E-stained sections of the rat thyroid gland of all experimental groups

[a, d] The control group demonstrates numerous follicles of different sizes loaded with acidophilic colloid (CI) and surrounded by connective tissue enclosing a normal amount of interfollicular cells (↑), blood capillaries (▶) and nerve fibers (NF), each follicle is lined by a single row of cuboidal follicular cells (FC) that have basophilic cytoplasm and rounded nuclei. [b,e] The furan group reveals collapsed follicles with little colloid (CI) and surrounded by connective tissue enclosing a large amount of interfollicular cells (↑),

congested blood capillaries and focal areas of hemorrhage (▶). Most of the follicles displayed multiple layers (blue arrow) of follicular cells, other follicles displayed disruption of their basal lamina with focal loss of the epithelial cells and communication (↔) with the adjacent follicles. [c, f] The Furan/Se group discloses many follicles that are distended with colloid (Cl) and few follicles have little amount. The blood capillaries (▶) in the surrounding connective tissue are not congested and a moderate amount of interfollicular cells (↑) is noticed. Some follicles reveal arranged follicular cells (FC) in a single layer while others showed focal areas of follicular cell proliferation (blue arrow). Scale bar of a, b, c =200µm (H&E staining x100) and scale bar of d,e,f =50µm (H&E staining x400).

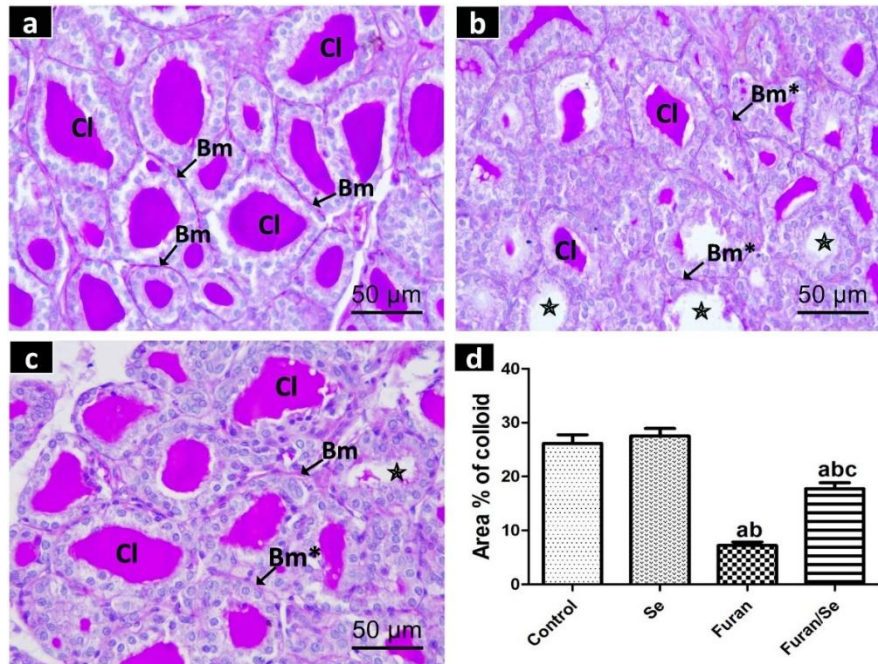


Figure 2. Photomicrographs of PAS-stained sections of the rat thyroid gland of all experimental groups

[a] The control group illustrates prevalent PAS-positive reaction in the colloid (Cl) and basement membranes (Bm) of almost all thyroid follicles. [b] The furan group displays PAS-positive reaction in few follicles having little amount of colloid (Cl) and also in the discontinuous basement membranes (Bm*) of some disrupted follicles, however many follicles have no colloid (*). [c] The Furan/Se group exhibits PAS-positive reaction in the colloid (Cl) and basement membranes (Bm) of most follicles and also in discontinuous basement membranes (Bm*) of some disrupted follicles. Moreover, few follicles have no colloid (*). Scale bar of a,b,c=50µm (PAS staining x400). [d] A Bar Graph revealing the area % of colloid in all experimental groups. Data are expressed as Mean±SD. The statistical analysis was performed using one-way ANOVA followed by the post hoc Tukey's test. ^a significant when compared to the control group. ^b significant when compared to Se group. ^c significant when compared to furan group.

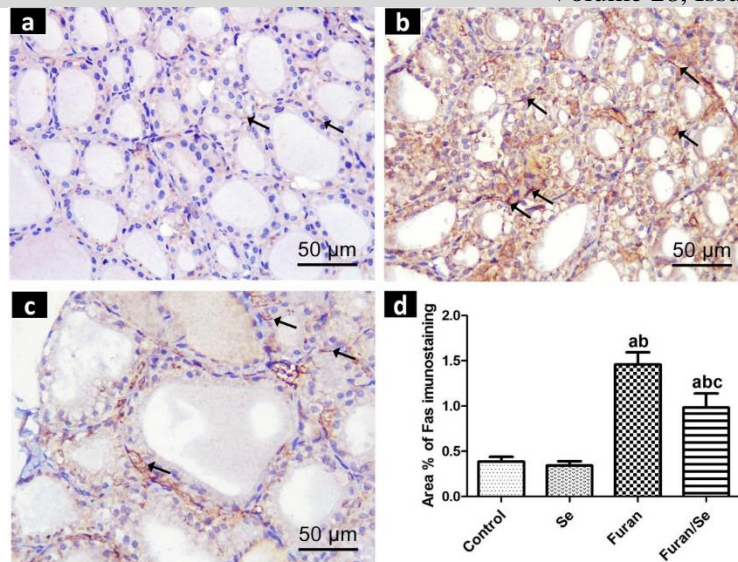


Figure 3. Photomicrographs of FAS-stained sections of the rat thyroid gland of all experimental groups

[a] The control group reveals a weak Fas immunoreactivity in the cell membranes (↑) of few follicular cells. [b] The furan group exhibits an extensive Fas immunostaining in the cell membranes (↑) of many follicular cells. [c] The Furan/Se group demonstrates a moderate Fas immunoeprssion in the cell membranes (↑) in a small number of follicular cells. Scale bar of a,b,c =50μm (FAS immunostaining x400). [d] A Bar Graph showing the area % of FAS immunostaining of all experimental groups. Data are expressed as Mean±SD. The statistical analysis was performed using one-way ANOVA followed by the post hoc Tukey's test. ^a significant compared to the control group. ^b significant compared to Se group. ^c significant compared to furan group.

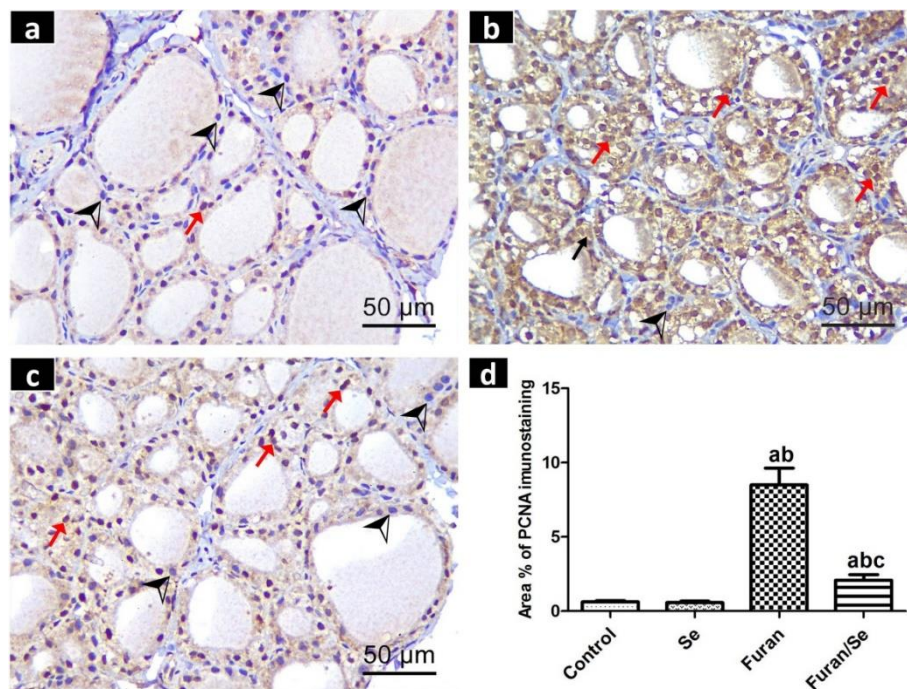


Figure 4. Photomicrographs of PCNA-stained sections of the rat thyroid gland of all experimental groups

[a] The control group demonstrates PCNA-negative immunoreactivity (▲) in a large number of follicular nuclei, however PCNA-positive immunoeprssion (red arrow) is noticed in few nuclei of other follicular epithelium [b] The furan group displays PCNA-positive immunoeprssion (red arrow) in numerous nuclei of the follicular epithelium and in proliferated interfollicular cells (black arrow), however few follicular nuclei display PCNA-negative immunoreactivity (▲). [c] The Furan/Se group exhibits PCNA-positive immunoeprssion (red arrow) in small number of nuclei of the follicular epithelium, however many follicular nuclei display PCNA-negative immunoreactivity (▲). Scale bar of a,b,c=50μm (PCNA

immunostaining x400). [d] A Bar Graph showing the area % of PCNA immunostaining of all experimental groups. Data are expressed as Mean \pm SD. The statistical analysis was performed using one-way ANOVA followed by the post hoc Tukey's test. ^a significant compared to the control group. ^b significant compared to Se group. ^c significant compared to furan group.

DISCUSSION

Furan, an endocrine disruptor chemical formed inevitably during thermal processing of most food, has warranted the scientists' great concern in recent years due to its potential disastrous effects to various mammalian tissues. In this study, exposure of adult male rats to oral furan for four consecutive weeks produced remarkable histopathological changes in the cytoarchitecture of the thyroid gland that displayed shrunken thyroid lobules with collapsed follicles and partially depleted thyrocolloid. The proposed mechanism of these deleterious histological changes could be attributed to furan-induced oxidative stress. Oxidative stress is defined as a disturbance in the balance between antioxidant defenses and the production of reactive oxygen species (ROS) that ultimately oxidize the polyunsaturated fatty acids and phospholipids in the mammalian cell, nuclear and mitochondrial membranes, resulting in generation of toxic lipid peroxidation products such as MDA [28].

In order to explore this potential effect of furan in inducing oxidative stress, besides measuring serum MDA, we have measured the non-enzymatic antioxidant (GSH) and assessed the level of activity of the enzymatic antioxidant (GPX-1). The furan group exhibited redox imbalance with increased MDA and decreased both GSH and GPX-1. In alignment with our results, furan administration in animals has been associated with not only increased serum and tissue levels of MDA and a significant decrease of GSH and GPX-1 but also, was accompanied with a decrease in glutathione-S-transferase (GST), catalase (CAT) and superoxide dismutase (SOD) [15- 18].

The decline in serum GSH "the body's master intracellular non-enzymatic antioxidant and the active coenzyme for the enzyme GPX-1" was probably due to its covalent bonding with cis-2-butene-1,4-dialdehyde (BDA) which is the primary metabolite of furan formed under the metabolic influence of the liver enzyme cytochrome P450 2E1 (CYP2E1) [7]. BDA is a highly cytotoxic reactive compound that binds irreversibly to proteins, amino acids, nucleosides and DNA [1, 29]. Consequently, these cellular nucleophilic molecules underwent irreversible

post-translational protein modification and lost their proper function [30].

In this study, GPX-1 enzyme was chosen, in particular, because it is abundantly expressed in the thyroid follicles and exerts a vital function in catalyzing the polymerization of the thyroglobulin colloid to its highly cross-linked storage form [31]. Therefore, the obtained decline in serum GPX-1 activity in furan-treated group could be beyond what we have observed in PAS-stained thyroid sections in that group; where the colloid was somewhat depleted; an outcome that might reflected upon the functional integrity of the thyroid gland with subsequent impeding of thyroid hormones (THs) biosynthesis following furan administration.

This hypothyroid impact of furan could be the possible cause behind the concomitant decline of serum total T3, T4 and increased TSH in a negative feedback loop; an event tightly regulated by the hypothalamic-pituitary-thyroid (HPT) axis. There is substantial evidence that furan cause hypothyroidism in exposed animals [32]. Being, an endocrine disruptor chemical, furan not only disrupted the reproductive system [8,19], but there is increasing evidence from animal and in vitro studies that the thyroid is also vulnerable to furan's endocrine-disrupting effects [10,11]. The exact mechanism of action of furan in impeding THs biosynthesis is unsettled, however several mechanisms are postulated in "inhibiting HPT axis at different cellular levels" including TSH receptors, iodide uptake, Na⁺/I⁻ symporter (NIS), thyroperoxidase (TPO), binding to transport proteins, thyroid receptors (TR α and TR β), nuclear transcription machinery, peripheral metabolism by THs iodothyronine deiodinases (DIO) or clearance by the liver [32]. Another postulated mechanism of the hypothyroid effect of furan is that some furan congeners, like polychlorinated dibenzofurans (PCDFs), have a high degree of structural resemblance to THs and therefore interfere with their binding to the transport proteins or to the thyroid receptors that, in turn, lead to subclinical hypothyroidism [33].

Pronouncedly, in Furan/Se group, concomitant administration of Se with furan could partially ameliorated the aforementioned-histological changes in the thyroid gland, counteracted the obtained redox imbalance and restored the serum

THs levels approximately back to the control level. This anticipatory role of Se was emanated from its incorporation in selenocysteine that forms the active center and the cofactor of about 25 selenoproteins which mediate most Se effects. Among these seleno-proteins are the seleno-enzymes which are highly expressed in the thyrocytes and include the GPXs, thioredoxin reductases (TRX-R) and the iodothyronine DIO families [21, 34].

The beneficial role of these seleno-enzyme families to the thyroid gland has been outstandingly announced. First, GPXs, particularly GPX-1, are a family of cytosolic enzymes that catalyze the reduction of hydrogen peroxide that is instantaneously released inside the colloid to be used normally by TPO enzyme for iodide organification during THs biosynthesis [35]. Second, TRX-R reduce the thioredoxins (TRX) which are a family of redox proteins lodged inside the thyroid in an oxidized and reduced form. The later form acts as an electron donor that participates in many NADPH-dependent redox signaling reactions [36]. Third, iodothyronine DIO are a family of membrane-bound enzymes that selectively remove iodide from thyroxine and its derivatives, thus activating these hormones [37].

It is noteworthy that, in the furan-treated group, furan toxicity was linked not only to its oxidative stress and hypothyroid impacts, but also was linked to the inflammatory effect induced by its active metabolite "BDA" which causes tissue toxicity and damage [9]. This inflammatory response was evident from the observed congested blood capillaries and focal areas of hemorrhage in some follicles in the furan-treated group that implied an ongoing inflammatory reaction and could be another proposed mechanism of the obtained histopathological changes of the thyroid gland in the rats of this group. This furan-provoked inflammation was confirmed and substantiated by statistical significant increase of the serum proinflammatory cytokines viz., IL-1 β and TNF- α . In line with these finding, Selmanoğlu et al. [38] and Yuan et al., [39] have documented an immense proinflammatory effect of furan with uprising of IL-1 β and TNF- α levels in rodent tissues.

In the present study, there was also an extensive immunoexpression of Fas receptor protein on the cell membrane of the follicular cells of the furan-treated rats together with increased the mean area % of Fas immunoreactivity compared to the control rats. These results might implicate upregulating effect of furan on the Fas receptors

that are also known "death receptors" and this might evince the increased liability of the follicular cells for apoptosis following furan administration. This high apoptotic liability could explain the emerged collapsed thyroid follicles with decreased their colloid content that was ascertained under light microscope in the furan group.

Actually, there are two proapoptotic proteins which are the dominators of the extrinsic apoptotic pathway viz., Fas ligand/Fas (FasL/Fas). The Fas (CD95), a transmembrane protein that belongs to the TNF receptor family, is constitutively expressed on the cell surface of almost all cells. On the other hand, the FasL (CD95L), a transmembrane protein belong to TNF family of proteins, is expressed mainly on activated cytotoxic T-lymphocytes. Binding of FasL with Fas receptors on the cell membrane trigger activation of intracellular death domain (DD) that interacts with a Fas-associated death domain protein (FADD) and the later triggers the activation of the caspases cascade from "the initiator caspase-8" to the "effector caspase-3" that finally leads to programmed cell death of the target Fas-expressing cells [40].

At the molecular level, there is bidirectional crosstalk between the inflammatory cytokines (IL-1 β & TNF- α) and (FasL/Fas) that appeared in triggering of the formers to the apoptotic signaling pathway of the later via sensitizing the Fas to its ligand FasL or via activating caspase-8 directly [40]. By virtue of this interplay, it was found that inflammatory cytokines facilitated the apoptotic destruction of thyroid follicular cells in experimental autoimmune thyroiditis [41]. Paradoxically, in a vicious circle fashion, Fas receptors activation leads to production of a storm of cytokines and chemokines [42].

Efficiently in the Furan/Se group, Se decreased the serum level of both IL-1 β and TNF- α and down regulated the Fas immunoexpression; consequences that implied an anti-inflammatory and anti-apoptotic competency of Se, respectively. Actually, the thyroid gland has an expontially high Se content and emerging evidence has highlighted that this tremendous amount of Se could inhibit many inflammatory cell mechanisms through its incorporation in variable seleno-enzymes [43]. Also, Se could suppress apoptosis via its incorporation into TRX-R enzymes that inhibit the release of cytochrome c, one of the major clue signals of apoptosis, from the mitochondria to the cytosol [35].

In the present work, an astonishing H&E finding was obtained disclosing the thyroid follicles with

multiple layers of follicular cells along with the IHC finding that displayed an extensive PCNA immunoexpression and a significant increase in the mean area % of PCNA immunoreactivity in furan-treated group. These findings pointed mostly to the furan-induced nuclear proliferation and might imply hyperplasia of the follicular cells as previously adopted by Gill et al. [10]. This proliferative effect of furan could be secondary to the oxidative stress developed after its long exposure that subsequently accentuated the proliferative drive of the cells [44]. Moreover, the proliferative effect might be attributed indirectly to the upregulating effect of furan to the inflammatory cytokines. In that concern, it was authorized that the inflammatory cytokines act, on long term, via multiple signal transduction pathways in expressing different genes that initiate cell proliferation, angiogenesis, tumor development and progression [45].

Intriguingly, in the last decades, International Agency for Research on Cancer (IARC) categorized furan as "Group 2B possible human carcinogen"[11]. In conjunction with that, previous carcinogenicity studies have suggested that furan acted by both genotoxic and non-genotoxic mechanisms, however, the precise conclusion concerning this issue remain elusive [14]. There is much evidence for the involvement of the furan intermediate metabolite "BDA" that binds covalently to DNA leading ultimately to epigenetic changes and hyperplasia [9]. Also, BDA forms DNA single-strand breaks, DNA-protein cross-links and DNA adducts in mammalian cells that intermingled together yielding abnormal transcription and replication and may be mutations which are depicted as precancerous attributes [18,46,47].

Finally, in this study, Se advocated anti-proliferative potential as was evident from the emerged results of Furan/Se group that exhibited a weak immunoexpression of PCNA and a significant decline in its mean area % in PCNA immunostained sections of the thyroid gland. Of particular interest, sodium selenite is one of the well-known derivatives of Se, together with seleno-L-methionine (SeMet) and Se-Methyl-selenocysteine (SeMCys), are responsible for the chemoprevention against carcinogenesis because of their ability to protect cellular molecules through redox-cycling [48].

CONCLUSION

Furan has detrimental effects on the cytoarchitecture of the rat thyroid gland that were partially mitigated by Se. Broadcasting educational measures must be implemented to

raise human' awareness about the toxicity of furan and enforce the notion to the heat-processed-food consumers for improving their Se status.

- Conflict of Interest: None.
- Financial Disclosures: None.

REFERENCES

- 1- Crews C, Castle L. A review of the occurrence, formation and analysis of furan in heat-processed foods. *Trends in Food Science & Technology*. 2007; 18(7): 365–72.
- 2- US Food and Drug Administration. Exploratory Data on Furan in Food. Washington, DC: FDA. 2004. Available at: <http://www.cfsan.fda.gov/about~dms/furandat.html>.
- 3- Bakhiya N, Appel KE. Toxicity and carcinogenicity of furan in human diet. *Archives of Toxicology*. 2010; 84(7): 563–78.
- 4- Becalski A, Hayward S, Krakalovich T, Pelletier L, Roscoe V, Vavasour E. Development of an analytical method and survey of foods for furan, 2-methylfuran and 3-methylfuran with estimated exposure. *Food Addit Contam Part A Chem Anal Control Expo Risk Assess*. 2010; 27:764–75.
- 5- Morehouse K, Nyman P, McNeal T, Dinovi M, Perfetti G. Survey of furan in heat processed foods by headspace gas chromatography/mass spectrometry and estimated adult exposure. *Food Addit Contam*. 2008; 25:259–64
- 6- Hamadeh H K, Jayadev S, Gaillard ET, Huang Q, Stoll R, Blanchard K, et al. Integration of clinical and gene expression endpoints to explore furan-mediated hepatotoxicity. *Mutation Research/Fundamental and Molecular Mechanisms of Mutagenesis*. 2004; 549(1-2): 169-83.
- 7- Alizadeh M, Barati M, Saleh-Ghadimi S, Roshanravan N, Zeinalian R, Jabbari M. Industrial furan and its biological effects on the body systems. *Journal of Food Biochemistry*. 2018; 42(5): e12597.
- 8- Rehman H, Jahan S, Ullah I, Winberg S. Toxicological effects of furan on the reproductive system of male rats: An "in vitro" and "in vivo"-based endocrinological and spermatogonial study. *Chemosphere*. 2019; 230: 327-36.
- 9- Knutsen HK, Alexander J, Barregård L, Bignami M, Brüschweiler B, Wallace H. Risks for public health related to the presence of furan and methylfurans in food. *EFSA Journal*. 2017; 15(10): e05005.
- 10- Gill S, Bondy G, Lefebvre D, Becalski A, Kavanagh M, Hou Y, et al. Subchronic oral

- toxicity study of furan in Fischer-344 rats. *Toxicol Pathol.* 2010; 38:619–30.
- 11- Gill S, Kavanagh M, Barker M, Weld M, Vavasour E, Hou Y, et al. Subchronic oral toxicity study of furan in B6C3F1 mice. *Toxicologic Pathology.* 2011; 39(5):787-94.
 - 12- Wang E, Chen F, Hu X, Yuan Y. Protective effects of apigenin against furan-induced toxicity in mice. *Food & function.* 2014; 5(8): 1804-12.
 - 13- Saracoğlu G, Baş H, Pandır D. Furan-induced cardiotoxicity in diabetic rats and protective role of lycopene. *Journal of food biochemistry.* 2019; 43(3): e12738.
 - 14- NTP "National Toxicology Program". Toxicology and carcinogenesis studies of furan (CAS No. 110–00-9) in F344/N rats and B6C3F1 mice (gavage studies). In: NTP Technical Report Series. 1993; No. 402. Research Triangle Park, NC: USA.
 - 15- IARC "International Agency for Research on Cancer". Summaries and Evaluations. 1995; Available at: <http://www.inchem.org/documents/iarc/vol63/furan.html>.
 - 16- Bas H, Pandır D. Protective effects of lycopene on furan-treated diabetic and non-diabetic rat. *Environ Sci.* 2016; 29:143–7.
 - 17- Kaya E, Yılmaz S, Ceribasi S. Protective role of propolis on low and high dose furan-induced hepatotoxicity and oxidative stress in rats. *Journal of Veterinary Research.* 2019; 63(3): 423-31.
 - 18- Russo MT, De Luca G, Palma N, Leopardi P, Degan P, Cinelli S, et al. Oxidative Stress, Mutations and Chromosomal Aberrations Induced by In Vitro and In Vivo Exposure to Furan. *International Journal of Molecular Sciences.* 2021; 22(18): 9687.
 - 19- Rehman H, Jahan S, Ullah I, Thörnqvist PO, Jabbar M, Shoab M et al. Effects of endocrine disruptor furan on reproductive physiology of Sprague Dawley rats: An F1 Extended One-Generation Reproductive Toxicity Study (EOGRS). *Human & Experimental Toxicology.* 2020; 39(8): 1079-94.
 - 20- Karacaoğlu E, Selmanoğlu G, Kilic A. Histopathological effects of the food contaminant furan on some endocrine glands of prepubertal male rats. *Turkish Journal of Medical Sciences.* 2012; 42(Sup. 1): 1207-13.
 - 21- Lossow K, Schwerdtle T, Kipp A. Selenium and iodine—essential trace elements for the thyroid. *Ernahr. Umsch.* 2019; 66: 175-80.
 - 22- Gorini F, Sabatino L, Pingitore A, Vassalle C. Selenium: An Element of Life Essential for Thyroid Function. *Molecules.* 2021; 26(23): 7084.
 - 23- Zachara BA. Selenium in complicated pregnancy: a review. *Adv Clin Chem.* 2018; 86:157–78.
 - 24- Swathy SS, Panicker S, Indira M. Effect of exogenous selenium on the testicular toxicity induced by ethanol in rats. *Ind. J Physiol. Pharmacol.* 2006; 50(3):215-24.
 - 25- Bancroft JD, Layton C. The hematoxylin and eosin. Chapter 10, pp. 126–137 and Carbohydrates. Chapter 13 pp 181-184. In: Suvarna, S.K., Layton, C., Bancroft, J.D. (Eds.), *Theory and Practice of Histological Techniques*, 2019; seventh ed. Churchill Livingstone Elsevier, Philadelphia, PA.
 - 26- Ramos-Vara JA, Miller MA. When Tissue Antigens and Antibodies Get Along: Revisiting the Technical Aspects of Immunohistochemistry—The Red, Brown, and Blue Technique. *Vet. Pathol.* 2014. 51: 42-87.
 - 27- Stehlik-Barry K, Babinec AJ. Comparing means and ANOVA. *Data Analysis with IBM SPSS Statistics.* Packt Publishing Ltd. 2017; pp. 229–65.
 - 28- Baş H, Kalender Y, Pandır D, Kalender S. Effects of lead nitrate and sodium selenite on DNA damage and oxidative stress in diabetic and non-diabetic rat erythrocytes and leucocytes. *Environ Toxicol Pharmacol.* 2015; 39:1019–26.
 - 29- Bolger P, Michael T, Shirley SH, Dinovi M. Hazards of dietary furan. *Process-Induced Food Toxicants: Occurrence, Formation, Mitigation, and Health Risks.* 2009; 117–33.
 - 30- Ramm S, Limbeck E and Mally A. Functional and cellular consequences of covalent target protein modification by furan in rat liver. *Toxicology.* 2016; 361: 49–61.
 - 31- Schmutzler C, Mentrup B, Schomburg L, Hoang-Vu C, Herzog V, Köhrle, J. Selenoproteins of the thyroid gland: expression, localization and possible function of glutathione peroxidase 3. *Biological Chemistry.* 2007; 1053-59.
 - 32- Boas M, Feldt-Rasmussen U, Skakkebak NE, Main KM. Environmental chemicals and thyroid function. *European Journal of Endocrinology.* 2006; 154(5): 599-611.
 - 33- Turyk ME, Anderson HA, Persky VW. Relationships of thyroid hormones with polychlorinated biphenyls, dioxins, furans, and DDE in adults. *Environmental health perspectives.* 2007; 115(8): 1197-203.

- 34- Bermingham EN, Hesketh JE, Sinclair BR, Koolaard JP, Roy NC. Selenium-enriched foods are more effective at increasing glutathione peroxidase (GPX-1) activity compared with selenomethionine: A meta-analysis. *Nutrients*. 2014; 6(10): 4002-31.
- 35- Leoni SG, Kimura ET, Santisteban P, De la Vieja A. Regulation of thyroid oxidative state by thioredoxin reductase has a crucial role in thyroid responses to iodide excess. *Molecular endocrinology*. 2011; 25(11): 1924-35.
- 36- Lincoln DT, Al-Yatama F, Mohammed FM, Al-Banaw AG, Al-Bader M, Burge M, et al. Thioredoxin and thioredoxin reductase expression in thyroid cancer depends on tumour aggressiveness. *Anticancer research*. 2010; 30(3): 767-75.
- 37- St. Germain DL, Galton VA, Hernandez A. Defining the roles of the iodothyronine deiodinases: current concepts and challenges. *Endocrinology*. 2009; 150(3): 1097-107.
- 38- Selmanoğlu G, Karacaoğlu E, Kılıç A, Kockaya EA, Akay MT. Toxicity of food contaminant furan on liver and kidney of growing male rats. *Environmental Toxicology*. 2012; 27: 613-22.
- 39- Yuan Y, Wang Z, Nan B, Yang C, Wang M, Ye, et al. Salidroside alleviates liver inflammation in furan-induced mice by regulating oxidative stress and endoplasmic reticulum stress. *Toxicology*. 2021; 461: 152905.
- 40- Rex J, Lutz A, Faletti LE, Albrecht U, Thomas M, Bode JG, et al. IL-1b and TNFa Differentially Influence NF-kB Activity and FasL-induced Apoptosis in Primary Murine Hepatocytes During LPS-Induced Inflammation. *Frontiers in Physiology* February. 2019;10 (117):1-16.
- 41- Wang SH, Bretz JD, Phelps E, Mezosi E, Arscott PL, Utsugi S, et al. A unique combination of inflammatory cytokines enhances apoptosis of thyroid follicular cells and transforms nondestructive to destructive thyroiditis in experimental autoimmune thyroiditis. *The Journal of Immunology*. 2002; 168(5): 2470-74.
- 42- Altemeier WA, Zhu X, Berrington WR, Harlan JM, Liles WC. CD95 (FAS) induces macrophage proinflammatory chemokine production via a MyD88-dependent, caspase-independent pathway. *J Leukoc Biol* 2007; 82:718-21.
- 43- Forceville X. Seleno-enzymes and seleno-compounds: the two faces of selenium. *Critical Care*. 2006; 10(6): 1-2.
- 44- Hickling KC, Hitchcock JM, Oreffo V, Mally A, Hammond TG, Evans JG, et al. Evidence of oxidative stress and associated DNA damage, increased proliferative drive, and altered gene expression in rat liver produced by the cholangiocarcinogenic agent furan. *Toxicol. Pathol.* 2010; 38: 230-43.
- 45- Hirano T. IL-6 in inflammation, autoimmunity and cancer. *International immunology*. 2021; 33(3): 127-48.
- 46- Byrns MC, Vu CC, Neidigh JW, Abad JL, Jones RA, Peterson LA. Detection of DNA adducts derived from the reactive metabolite of furan, cis-2-butene-1,4-dial. *Chem. Res. Toxicol.* 2006; 19: 414-20.
- 47- Ding W, Petibone DM, Latendresse JR, Pearce MG, Muskhelishvili L, White GA, et al. In vivo genotoxicity of furan in F344 rats at cancer bioassay doses. *Toxicol. Appl. Pharmacol.* 2012; 261:164-71.
- 48- Schröterová L, Králová V, Voráčová A, Hašková P, Rudolf E Červinka M. Antiproliferative effects of selenium compounds in colon cancer cells: Comparison of different cytotoxicity assays. *Toxicology in vitro*. 2009; 23(7): 1406-11.

mandour, D., Abdelfattah, M., Shuaib, D., Sabry, R. Cytoarchitecture changes of the rat thyroid gland following Furan administration implemented Fas-apoptotic pathway with potential abrogating role of selenium. *Zagazig University Medical Journal*, 2022; (871-882): -. doi: 10.21608/zumj.2022.129544.2537